Marine Structures 24 (2011) 358–376

Contents lists available at ScienceDirect

Marine Structures

journal homepage: www.elsevier.com/locate/marstruc

On the slack phenomena and snap force in tethers of submerged floating tunnels under wave conditions

Wei Lu, Fei Ge*, Lei Wang, Xiaodong Wu, Youshi Hong

State Key Laboratory of Nonlinear Mechanics, Institute of Mechanics, Chinese Academy of Sciences, No.15 Beisihuanxi Road, Beijing 100190, China

ARTICLE INFO

Article history:
Received 18 August 2010
Received in revised form 29 March 2011
Accepted 11 May 2011

Keywords:
Submerged floating tunnel
Tether slacking
Snap force
Bilinear oscillator
Structure parameter
Slack criterion

ABSTRACT

Under severe sea wave conditions, the mooring tethers of submerged floating tunnel (SFT) might go slack. It may cause the structure failure during the service lifetime of SFT. The paper investigated SFT dynamics when going through tether slacking and the related snap force under wave conditions. Besides the nonlinearity of fluid drag and of structural geometry for a relative large structure displacement, the problem is characterized by the nonlinearity due to the discontinuity in axial stiffness of the tethers. To include these nonlinearities, the method of Lagrange energy is used to build the governing equations of SFT motion, and a bilinear oscillator is introduced to simulate the mooring tether operating in an alternating slack-taut state. The sensitivities of the occurrence of tether slacking to wave height and wave period are investigated. Results show that at a large wave height SFT tether will go slack and snap force occurs. SFT responses are categorized into three types of state according to the dynamic response characteristics of tether tension. Effects of two fundamental structure parameters, buoyancy-weight ratio (BWR) and inclined mooring angle (IMA), on the dynamic responses of SFT are analyzed. A slack-taut map of SFT tethers is built. It intuitively describes the occurrences of slack and snap force with different combinations of the two parameters. An analytical approach for slack prediction by deriving the slack criterion is provided to reveal the mechanism of the presented slack-taut map. By present research, the authors tried to make their effort to provide an alternative philosophy for SFT structural design on concerning preventing the occurrence of tether slacking and snap force.

* Corresponding author. Tel.: +86 1082543968; fax: +86 1062561284.
E-mail address: gefei@imech.ac.cn (F. Ge).

0951-8339/$ – see front matter © 2011 Elsevier Ltd. All rights reserved.
doi:10.1016/j.marstruc.2011.05.003

1. Introduction

Submerged Floating Tunnel (SFT), also named Archimedes Bridge, is an innovative transportation concept for crossing straits, sounds, lakes or other kinds of waterways in general. As the name suggests, it is a tube-like structure floating at a certain depth in water supported by its self-buoyancy and constrained by mooring systems. An SFT mainly consists of four parts: (i) the tubes which are made up of tunnel segments and allow traffics and pedestrians to get through, (ii) the joints including those connecting the adjacent tunnel segments and the tunnel-shore connectors, (iii) the mooring systems which are anchored to the waterbed and keep the floating tunnel in position, (iv) the foundation constructed at the waterbed to install mooring systems.

Characterized as a submerged structure floating in the water, SFT has a lower impact on the local environment comparing to traditional bridges. Besides, the cost of SFT per unit length will not increase with the total span, which makes SFT an attractive option especially for deep or long waterway crossings [1–4]. SFT is exposed to many kinds of loads and potential hazards during its service life involving: (i) permanent loads encompassing structural weight and hydro-static pressure, (ii) environmental loads such as wind-induced waves, internal waves, currents, earthquakes etc., (iii) functional loads such as traffic loads and weight of ballast, (iv) accidental loads due to unexpected hazards such as internal explosion, fire, collision on the tunnel shell, loss of a mooring system, etc.

In some severe conditions such as a huge wave, earthquakes etc., SFT tethers might go slack. The occurrence of this phenomenon is due to the fact that the tether is highly resistible to tension while could hardly undertake compression. When the motion of tunnel goes large, the tension of SFT tethers might fall to a low level, and the tethers could become slack. In the cases of periodical excitation such as wind-induced wave, the tether will operate in alternating taut-slack conditions. Depending on the transition rate at which the tether becomes taut from slack state, it may cause very high tension in the tether which is referred to as “snap force” due to its impact effect [5–8].

Even though the original idea of SFT was conceived as early as 1880s [4], still there is no an SFT actually been built. Except for the social reasons, various scientific and technical difficulties are still in the way to realize it, such as fluid-structure-soil coupling, vortex induced vibration of tethers, the cable system configuration, the tunnel-shore joint design, etc. Many researches have been carried out so far.

Analytical study on dynamic response of a long SFT under wave condition was carried out in Ref. [9], and linear restoring force of mooring tethers was taken. Compressive force in the tethers was found in some cases, which meaned slack would happen in the tether. The nonlinearity due to catenary curve effect of mooring tether was considered in Ref. [10]. Comparison with linear restoring force reveals that this nonlinearity is not negligible unless for short tethers. If the ratio of leg weight to the net buoyancy of the tunnel is larger than 0.05, the linear assumption will underestimate the displacement and tether tension of SFT. Motohiro Sato et al. [11] idealized SFT as beam on elastic supports, and found that BOES (beams on equidistant elastic supports) could be modeled as BOEF (beams on elastic foundations) both for static and dynamic problems as long as the so-called relative stiffness of the supports $K_v \leq 0.05$. A finite element model accounting for geometrical nonlinearities and hydrodynamic loads was built to simulate the anchoring bars of SFT in Ref. [12]. The element was inserted in a step-by-step procedure for the numerical analysis of nonlinear response of SFT to seismic loading. In Ref. [13] this element was refined to extend its capabilities to full 3-D analysis and then implemented to the numerical procedure for full 3-D analysis of SFT under seismic and hydrodynamic excitation. Xu Long [3] took the structural design scheme of submerged floating tunnel prototype of Qiandao Lake in China as calculation model, and investigated the effects of structure parameters on dynamic responses of SFT under hydrodynamic loads. And the results indicated that the buoyancy-weight ratio (BWR) of SFT is a key structure parameter.

A series model experiments were carried out to investigate dynamic behaviors of SFT under regular waves in wave tank of the Hokkaido Development Ministry [14,15]. It is worth noting that tether slacking was observed for several mooring types of SFT; the dynamic tension of the tethers was no longer sinusoidal and snap force might occur under relatively severe wave conditions. Their results showed, for the case of tether perpendicular to sea-bed, the transverse displacement was significant but the snap force was almost negligible.

Although the previous work of numerical simulation has provided a profound insight into the dynamic behavior of SFT in various conditions, still it is not robust in many aspects. An important one is that most of the previous work has not considered the possible slack of the tethers. The necessity of the research of SFT tether slacking lies in two aspects mainly: for one aspect, on the design stage the structure configuration should be chosen to avoid the occurrence of tether slacking under the specified local load conditions; for another aspect, avoiding zero tension is actually unattainable for the unpredictability of all kinds of disasters, and may even be undesirable for underutilizing the tether as it is not clear how the slack condition will affect the dynamic behavior of the system.

SFT dynamics with the occurrence of tether slacking is characterized by the marked nonlinearity due to the discontinuity in the tether stiffness when shifting between the states of taut and slack. In this paper, a bilinear oscillator was introduced to simulate the mooring tether of SFT. As the structure might undergo a relative large motion when slack occurs, energy method was used to build the equations of motion so that the geometric nonlinearity of the structure can be fully considered. A numerical procedure was carried out to solve this nonlinear problem of multiple degrees of freedom. The sensitivity of slack to wave parameters and fundamental structure parameters was discussed. Finally an analytical approach to predict occurrence of SFT tether slacking was introduced by deriving the slack criterion.

2. Equations of motion

A single SFT segment moored by four tethers is considered as shown in Fig. 1. Several assumptions are made to simplify the problem: (i) the tunnel is assumed to be rigid in analysis as the deflection of the tunnel is small compared to the tether; (ii) the direction of fluid force is perpendicular to the axis of the tunnel, so that the motion of SFT is in plane; (iii) the drag force which the surrounding fluid exerts on the tether and lateral motion of the tether is neglected.

A bilinear oscillator is introduced to simulate the tethers. When taut, i.e. the instant length of the tether L_i ($i = 1,\ldots,4$) is larger than its unstrained length L_n, the stiffness of the tether is a constant value K_i. While when slack, i.e. the instant length of the tether is smaller than the unstrained length, the stiffness of the tether is zero. The Cartesian coordinate systems *oxy* and *cx'y'* are defined in Fig. 1. The *oxy* is a fixed coordinate system, of which the origin *o* is the midpoint of the line between the two mooring points on the mudline *BD* and the *x* -axis is parallel to the mudline. The *cx'y'* is the body fixed coordinate system, of which the origin *c* is the center of the tunnel cross section and the *x'* -axis is parallel to the line between two mooring points on the tunnel *AC*. Choose the coordinates of the origin of *cx'y'* in *oxy*, *xy*, and the rotation angle of *cx'y'* with respect to *oxy*, φ as the general coordinates. The system has 3 degrees of freedom. Lagrange equation is used to derive the governing equation. The kinetic energy of the system is given by:

$$KE = \frac{1}{2}m\left(\dot{x}^2 + \dot{y}^2\right) + \frac{1}{4}mR^2\dot{\varphi}^2 \tag{1}$$

in which m is the mass of the tunnel and R is the outer radius of the tunnel. The dots over the variables denote differentiation with respect to time.

The potential energy of the system is given by:

$$PE = -wy + \sum_{i}^{4}\frac{1}{2}K_i\Delta L_i^2 \tag{2}$$

where w is the redundant buoyancy of SFT and K_i is the stiffness of tether i, which can be expressed as:

$$K_i(\Delta L_i) = \begin{cases} k = \dfrac{EA_{tether}}{L_n}\,(\Delta L_i \geq 0), & \Delta L_i = L_i - L_n \quad i = 1,\ldots,4 \\ 0\,(\Delta L_i < 0) \end{cases} \tag{3}$$

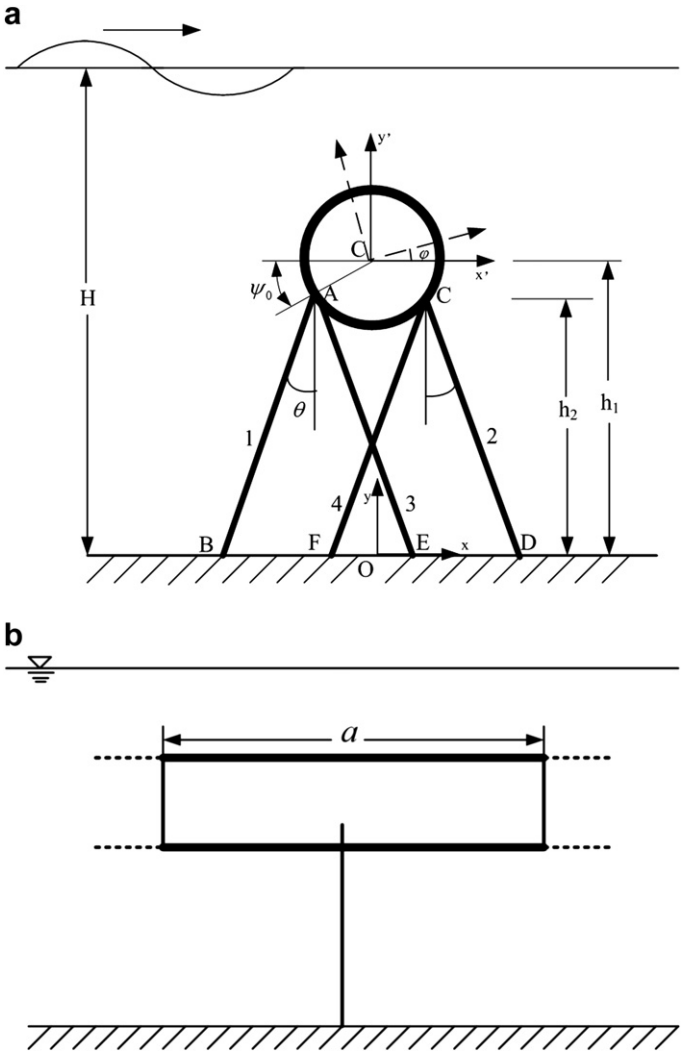

Fig. 1. Sketch of a single SFT segment moored by four tethers [9]. a. Cross-sectional view of SFT b. Side view of SFT.

Thus, the Lagrange function is given by:

$$L = KE - PE = \frac{1}{2}m\left(\dot{x}^2 + \dot{y}^2\right) + \frac{1}{4}mR^2\dot{\varphi}^2 + wy - \sum_i^4 \frac{1}{2}K_i\Delta L_i^2 \tag{4}$$

Substitution of this Lagrange function into the Lagrange equation (5) leads to:

$$\frac{d}{dt}\left(\frac{\partial L}{\partial \dot{q}_i}\right) - \frac{\partial L}{\partial q_i} = Q_i \tag{5}$$

in which q_i is the i-th general coordinate, and Q_i is the relevant nonconservative general force. So that the equations of motion are derived as:

$$\begin{cases} m\ddot{x}+\dfrac{1}{2}\sum_{i=1}^{4}K_i(\Delta L_i)\dfrac{\partial\left(\Delta L_i^2\right)}{\partial x}=f_x a \\ m\ddot{y}-\left(w-\dfrac{1}{2}\sum_{i=1}^{4}K_i(\Delta L_i)\dfrac{\partial\left(\Delta L_i^2\right)}{\partial y}\right)=f_y a \\ \dfrac{1}{2}mR^2\ddot{\varphi}+\dfrac{1}{2}\sum_{i=1}^{4}K_i(\Delta L_i)\dfrac{\partial\left(\Delta L_i^2\right)}{\partial \varphi}=f_\varphi a \end{cases} \tag{6}$$

in which f_x andf_y are respectively the fluid forces per unit length in x and y direction, f_φ is the rotational moment of fluid force per unit length, and a is the length of the tunnel segment.

The nonlinear restoring forces in Equations (6) can be expanded as:

$$\begin{aligned}
&\frac{1}{2}\sum_{i=1}^{4}K_i\frac{\partial\left(\Delta L_i^2\right)}{\partial x}=\sum_{i=1}^{4}K_i(L_i-L_n)\frac{\partial L_i}{\partial x}\\
&=K_1(L_1-L_n)\frac{x-R\cos(\varphi+\psi_0)+h_2\tan\theta+R\cos\psi_0}{L_1}+K_2(L_2-L_n)\frac{x+R\cos(\varphi-\psi_0)-h_2\tan\theta-R\cos\psi_0}{L_2}\\
&+K_3(L_3-L_n)\frac{x-R\cos(\varphi+\psi_0)-h_2\tan\theta+R\cos\psi_0}{L_3}\\
&+K_4(L_4-L_n)\frac{x+R\cos(\varphi-\psi_0)+h_2\tan\theta-R\cos\psi_0}{L_4}\\
&\frac{1}{2}\sum_{i=1}^{4}K_i\frac{\partial\left(\Delta L_i^2\right)}{\partial y}=\sum_{i=1}^{4}K_i(L_i-L_n)\frac{\partial L_i}{\partial y}\\
&=K_1(L_1-L_n)\frac{y-R\sin(\varphi+\psi_0)}{L_1}+K_2(L_2-L_n)\frac{y+R\sin(\varphi-\psi_0)}{L_2}+K_3(L_3-L_n)\frac{y-R\sin(\varphi+\psi_0)}{L_3}\\
&+K_4(L_4-L_n)\frac{y+R\sin(\varphi-\psi_0)}{L_4}\\
&\frac{1}{2}\sum_{i=1}^{4}K_i\frac{\partial(\Delta L_i)}{\partial \varphi}=\sum_{i=1}^{4}K_i(L_i-L_n)\frac{\partial L_i}{\partial \varphi}\\
&=R\Bigg\{K_1(L_1-L_n)\frac{[x-R\cos(\varphi+\psi_0)+h_2\tan\theta+R\cos\varphi_0]\sin(\varphi+\psi_0)-[y-R\sin(\varphi+\psi_0)]\cos(\varphi+\psi_0)}{L_1}\\
&+K_2(L_2-L_n)\frac{-[x+R\cos(\varphi-\psi_0)-h_2\tan\theta-R\cos\varphi_0]\sin(\varphi-\psi_0)+[y+R\sin(\varphi-\psi_0)]\cos(\varphi-\psi_0)}{L_2}\\
&+K_3(L_3-L_n)\frac{[x-R\cos(\varphi+\psi_0)-h_2\tan\theta+R\cos\varphi_0]\sin(\varphi+\psi_0)-[y-R\sin(\varphi+\psi_0)]\cos(\varphi+\psi_0)}{L_3}\\
&+K_4(L_4-L_n)\frac{-[x+R\cos(\varphi-\psi_0)+h_2\tan\theta-R\cos\varphi_0]\sin(\varphi-\psi_0)+[y+R\sin(\varphi-\psi_0)]\cos(\varphi-\psi_0)}{L_4}\Bigg\}
\end{aligned} \tag{7}$$

in which ψ_0 is the connecting angle of the mooring point and h_2 is the static height of the mooring point of SFT as shown in Fig. 1a.

Based on the modified Morison equation, the fluid force per unit length in Equations (6) can be written as:

$$\begin{aligned}
f_x &= \rho_w A\dot{w}_x+C_M\rho_w A\left(\dot{w}_x-\ddot{x}\right)+\frac{1}{2}\rho_w DC_D|w_x-\dot{x}|\left(w_x-\dot{x}\right)\\
f_y &= \rho_w A\dot{w}_y+C_M\rho_w A\left(\dot{w}_y-\ddot{y}\right)+\frac{1}{2}\rho_w DC_D|w_y-\dot{y}|\left(w_y-\dot{y}\right)
\end{aligned} \tag{8}$$

where ρ_w is the density of the fluid, A is the cross section area of SFT, D is the outer diameter of SFT,C_M is the coefficient of added mass, C_D is the drag coefficient, and w_x,w_y are velocities of water particles in x,y directions respectively. f_x,f_y are imposed along the axis of SFT, thus the rotational moment of fluid force f_φ=0. Linear Airy wave theory is taken to determine the velocity and acceleration of water particles.

For mild sea states, the displacement of the structure is small, so that the fluid force is generally calculated at the initial position. While in present study, a relatively severe sea state is considered and SFT might undergo a large displacement. The transient position of SFT varies greatly from the initial position, thus the velocity and acceleration of water particles is calculated in instant position of SFT.

The formulas of Equation (6) show that there are three sources of nonlinearity involved, that is the discontinuity in the tether stiffness, the geometry attribute (both of them are reflected in the term of restoring forces), and drag forces of fluid. Due to the nonlinear and coupled nature of the governing equations, analytic solutions are hard to pursue. In the following, the method of direct integration– the fourth order Runge-Kutta method is taken to solve the governing equations.

3. Analysis case

The conceptual design of SFT for Funka Bay, Hokkaido with a span of 30 km and a depth of 100 m in Japan [16] was taken as the analysis case in this paper. The designed SFT has a main body with four car lanes and two railway lanes. The design values of structure parameters and local environmental parameters specified by the Society of Submerged Floating Tunnel Technology Research in Hokkaido were used for the analysis conditions and were shown in Table 1 and Table 2. Fig. 2 shows the designed dimensions of cross section for assumed SFT. Several types of mooring line configuration were proposed, of which a four-tether type was considered in this paper. The discussion of present research is confined to a certain range of interest around the designed wave conditions and structure configurations.

4. Results and discussion

4.1. Effect of wave parameters

A series of wave height (5–15 m) and wave period (8–16 s), which cover the designed value as shown in Table 2, are considered with given structure parameters.

4.1.1. Effect of wave height

Fig. 3 shows time series of three typical dynamic responses of SFT tether tension force subjected to waves with different heights, in which T1 and T4 are tether tensions of No.1 and No.4 respectively, i.e. the outer tether and inner tether of the left side, as shown in Fig. 1a. When the wave height is small (as shown in Fig. 3a), the time series of SFT tether tension force is harmonic. Owing to the rotation of the tunnel, the dynamic amplitude of outer tethers (No.1 and No.2) tensions is greater than that of inner

Table 1
Structure parameters of conceptual design of Funka Bay SFT.

Classification	Item	Value
Tunnel Installation Depth (from top)		30 m
Length of a Single Tunnel Module		93.2 m
Tunnel Cross Section	Outside Diameter	23 m
	Wall Thickness	1 m
	Material	Concrete
	Weight in Air	2.88×10^6 N/m
	Buoyancy	4.25×10^6 N/m
	Drag Coefficient	1.0
	Added Mass Coefficient	1.0
Connection Angle Ψ_0		30°
Mooring Line	Tensile Stiffness	3.626×10^8 N/m

Table 2
Local environmental conditions of Funka Bay.

Span of Waterway	30 km
Water Depth	100 m
Significant Wave Height	9.3 m
Wave Period	13.0 s

tethers (No.3 and No.4). When the wave height increases, the response of tether tension will no longer be harmonic, but still be periodic. Once the wave height is as large as 12 m, the minimum tension force of outer tether will reach zero, which means the outer tether becomes slack. Fig. 3c shows that when the wave height rises as large as 14 m, the response of tether tension will no longer be periodic, and the dynamic amplitude of the outer tether will not necessarily be greater than the inner one. Both of the outer and the inner tethers will go slack. And the response of tether tension presents the following characteristics:

1. The maximum tether tension force is much larger than that of periodic ones (including non-slack and periodic slack responses).
2. The SFT tether alternately goes from slack to taut. While shifting, the tether tension force increases sharply to the peak in a short time, and then falls down to zero sharply, which appears the feature of impulse force.

The aforementioned two characteristics suggest that tension force has an impact effect to both the SFT and the tether, i.e. the so-called “snap force” occurs. According to the character of dynamic responses of SFT tether tension as described above, the state of SFT dynamic response can be categorized into three types: taut, slight slack and slack with snap force.

Fig. 4 shows the maximum and the minimum tension forces in SFT tethers, in which Fig. 4b is part of Fig. 4a when the wave height is smaller than 14 m. It suggests that SFT tethers will not go slack when the wave height is small, and the maximum and the minimum tension force will both vary with the wave height almost linearly. Even a slight slack (while 12 m $\leq$ wave height < 14 m) will not induce a significant increase in tether tension. However, when the wave height reaches 14 m, the maximum tension will increase to a large value, about 10 times of that of slight slack, which is fatal to SFT.

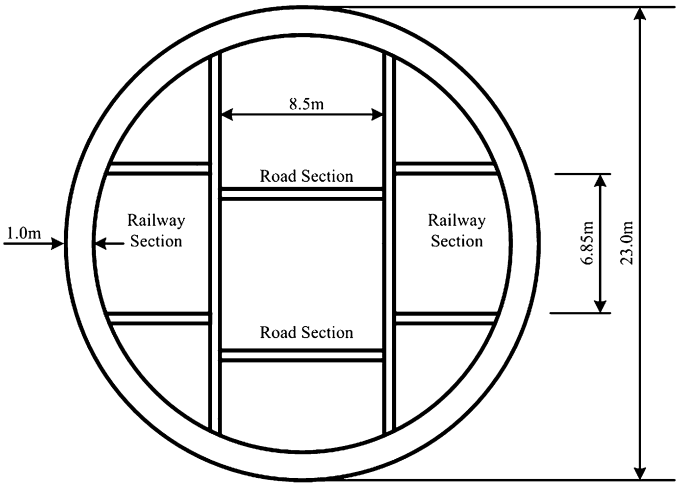

Fig. 2. Dimensions of Funka Bay SFT cross section [16].

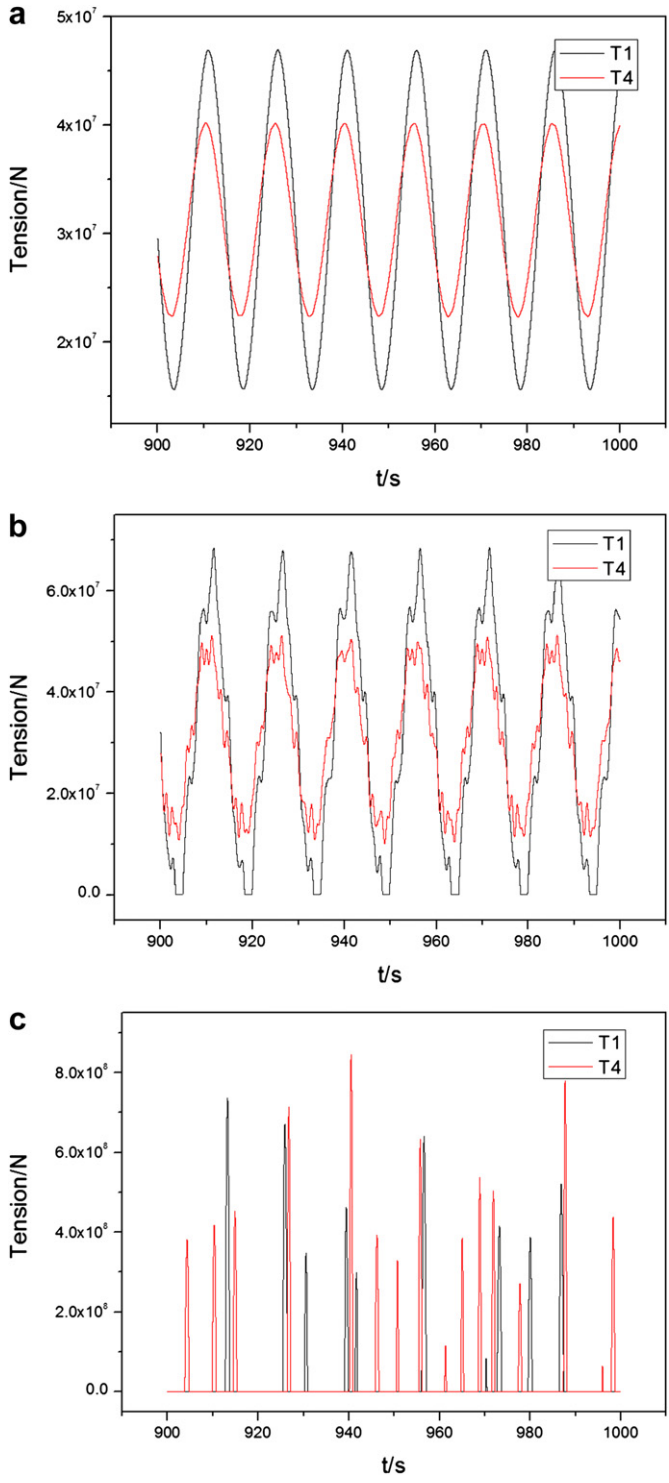

Fig. 3. Time series of typical responses of SFT tether tension force. a. wave height = 6 m, wave period = 15 s; b. wave height = 12 m, wave period = 15 s; c. wave height = 14 m, wave period = 15 s.

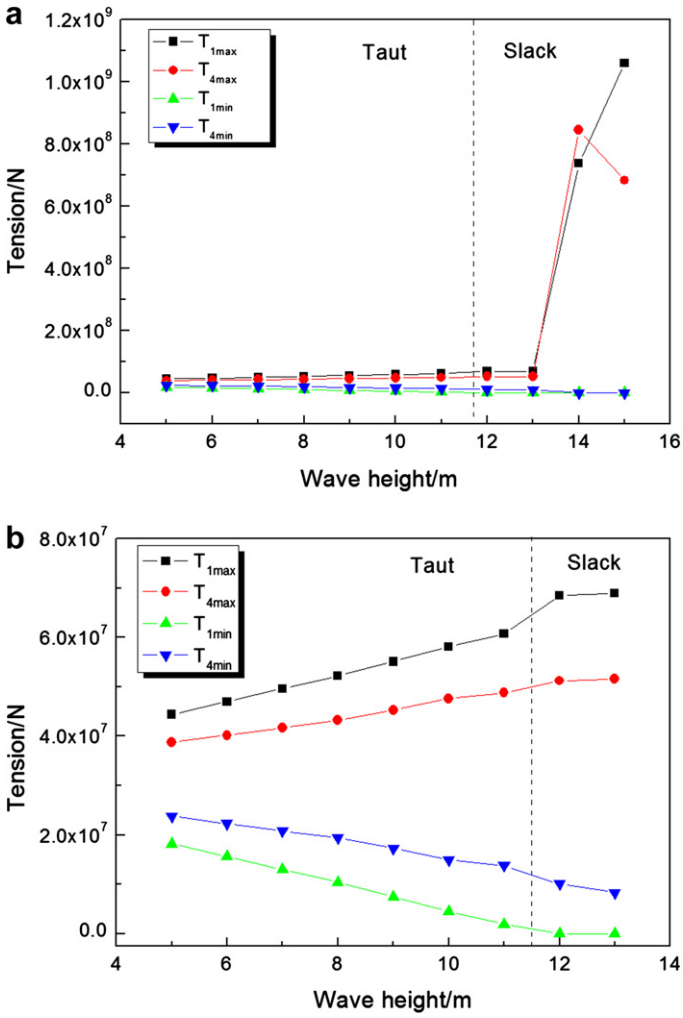

Fig. 4. Maximum and minimum tether tension force versus wave height.

4.1.2. Effect of wave period

Fig. 5 shows several typical dynamic responses of SFT tether tension under different wave periods. Slack does not occur. It is seen that the variation of the wave period will not change the characteristic of tension response of SFT tether, but only change the response frequency.

As shown in Fig. 6, when the wave period is small (8–11 s), the maximum and the minimum tether tension force will vary with the wave period almost linearly; whereas when the wave period is larger than 12 s, a further increase in wave period will not arouse a significant change in tether tension anymore. Thus, it indicates that in the range of concern, the influence of the wave period on SFT dynamic response is not as significant as the wave height.

4.2. Effects of structure parameters

Two fundamental structural parameters namely BWR and IMA are discussed. BWR, buoyancy-weight ratio, is defined as the ratio of buoyancy to the self weight of SFT. BWR is a key parameter of SFT

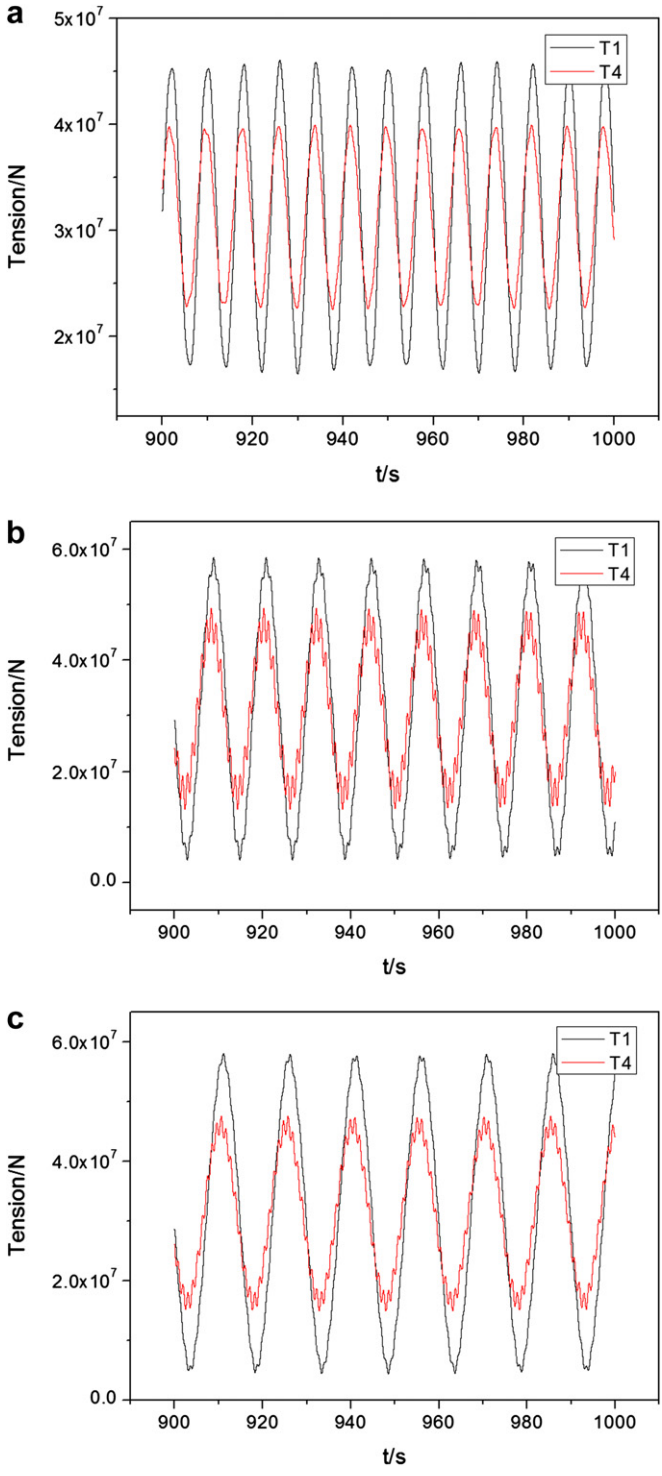

Fig. 5. Time series of typical responses of SFT tether tension force. a. wave height = 10 m, wave period = 8 s; b. wave height = 10 m, wave period = 12 s; c. wave height = 10 m, wave period = 15 s.

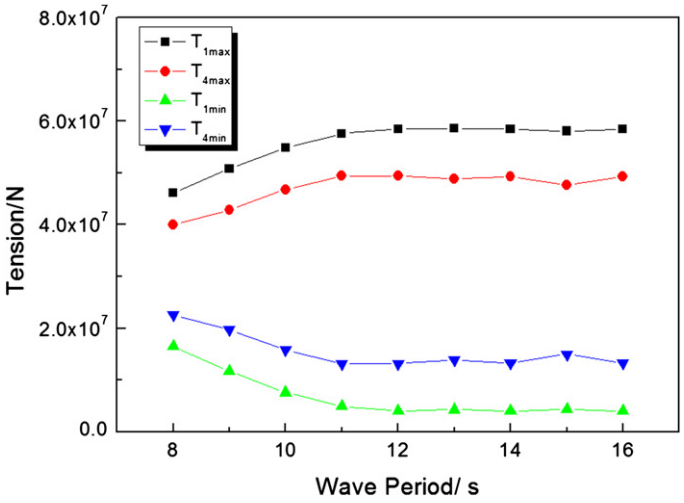

Fig. 6. Maximum and minimum tether tension force versus wave period.

[3], for it not only reflects the structure mass of SFT but also determines the initial tension force of the mooring system. As a submerged moored structure, mooring line arrangement is one of the main parts of SFT design. Inclined mooring angle (IMA), which is the initial angle between SFT tether and y -axis when SFT is at its equilibrium position, has a great influence on constraint of SFT and its natural frequency.

Effects of the two structure parameters are investigated under a relatively severe wave condition (wave height: 12 m, wave period: 15 s). Special attention is paid to the sensitivity of tether slacking to structure parameters.

4.2.1. Effect of BWR

A suitable value of BWR is desirable and should be given a profound consideration when design. For the consideration of structural stability, BWR should be large enough to provide sufficient redundant buoyancy. However it should not be too large to exert a high tension force in the tether. In present research, calculation is carried out with BWR varying in the range of 1.1–1.9 and a constant IMA of 30°.

It is seen from Fig. 7 that if BWR is smaller than 1.4, the outer tether will go slack; if BWR is smaller than 1.3 snap force will occur in tethers; whereas if BWR is larger than 1.4, SFT tethers will not go slack and the dynamic response of tether tension force is harmonic.

As shown in Fig. 8, if BWR is small (BWR < 1.4), SFT tether will go slack and the maximum tension force will be much larger than other conditions. When BWR reaches 1.4, only slight slack occurs. If BWR is larger than 1.4, the tether will no longer slack, and both of the maximum and minimum tension force will increase with BWR.

The dimensionless variable DT (relative dynamic tension amplitude) is introduced to eliminate the effect of initial tether tension. It is defined as: $\mathrm{DT} = (T_{\max} - T_0)/T_0$. Fig. 9 shows the relation between the value of DT with BWR, in which Fig. 9b is right part of Fig. 9a when BWR $\geq$ 1.4. It is seen that DT generally decreases with BWR, and the tendency is much more obvious when slack occurs. When the tethers remain taut (BWR > 1.4), DT is smaller than 1.

4.2.2. Effect of IMA

When inclined mooring angle θ varies from 0° to 45° with a constant BWR of 1.4, the relation of the maximum and the minimum tether tension force with θ is shown in Fig. 10, from which it is seen that if IMA is zero, the tethers will remain taut; once the angle is larger than zero, slack will occur; but if the angle reaches 30°, the tethers will remain taut again.

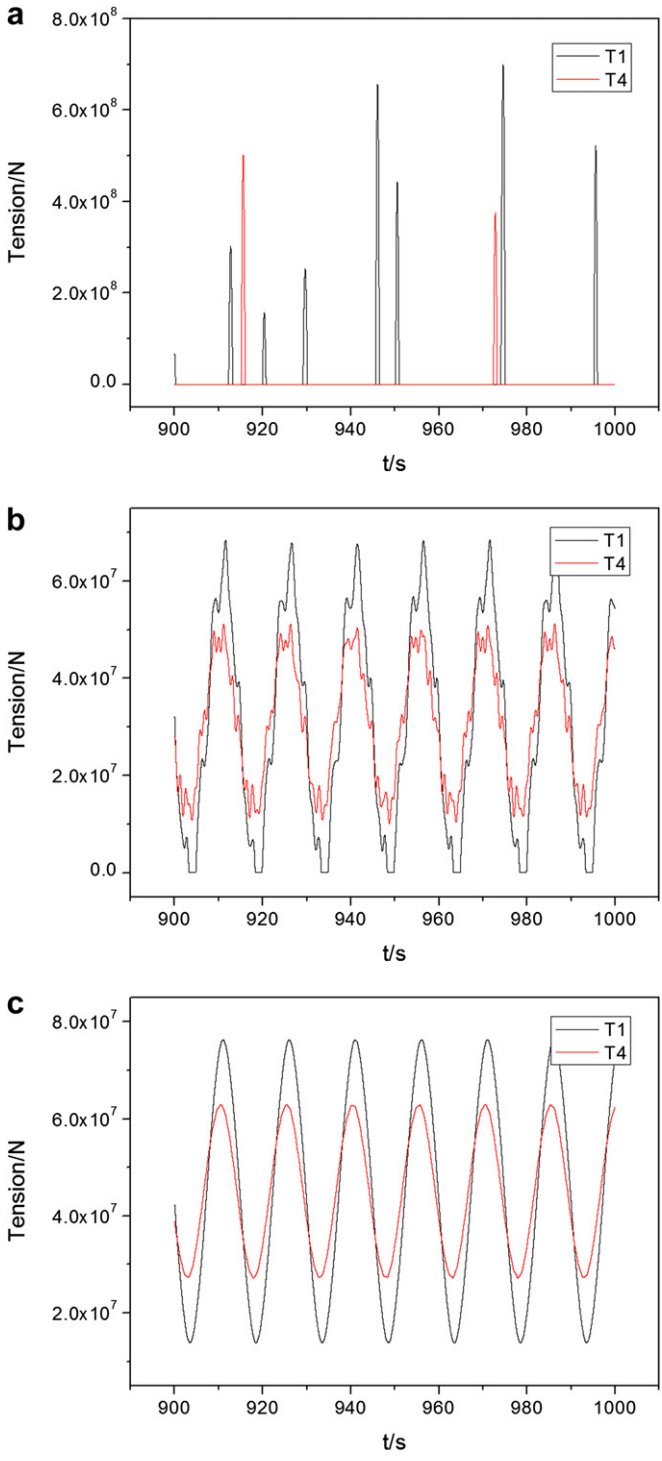

Fig. 7. Time series of typical tension responses of SFT tethers at different BWRs. a. BWR = 1.1; b. BWR = 1.4; c. BWR = 1.7.

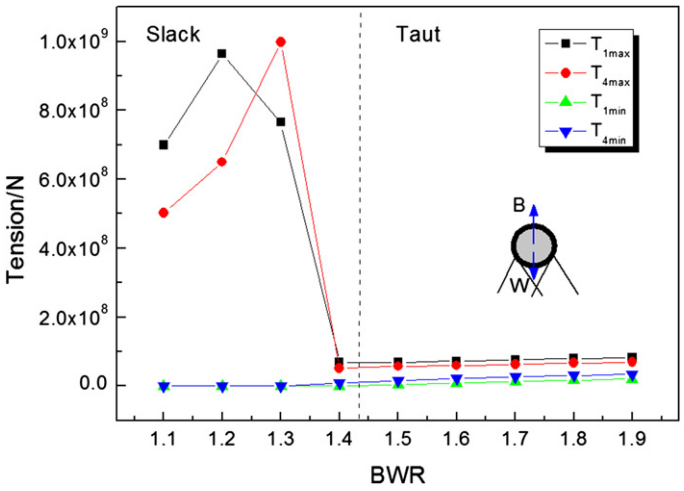

Fig. 8. Maximum and minimum tether tension force versus BWR.

Likewise, DT is introduced to reflect the influence of IMA, as shown in Fig. 11. It can be seen that DT increases sharply with θ firstly, and then keeps decreasing. If θ is larger than 30°, the tendency will be much milder. DT reaches a peak value around an IMA of 15°.

4.2.3. Slack-taut map of SFT tether

Further calculations of deferent combinations of BWR and IMA were carried out. Thus a slack-taut map of SFT tether, which decides whether slack will occur or not, is obtained. According to the character of dynamic tensions of SFT tether described in 4.1.1, the states of SFT dynamic response are divided into three types: taut, slight slack in the tether, and slack with snap force in the tether, which correspond to black, red hollow and red solid dots in Fig. 12 respectively.

Fig. 12 shows that the slack of SFT tether is sensitive to both BWR and IMA, while BWR determines the range of influence of IMA. When BWR is large, the range is narrow and slack mainly occurs around an IMA of 10° and the range will go widened as BWR decreases. When BWR is as small as 1.1, slack will occur in all the cases despite of a varying IMA in this specified wave condition. It is worth noting that an IMA of zero is very special that SFT tethers do not go slack for all BWR values larger than 1.1.

The slack-taut map directly shows the affecting pattern of BWR and IMA. Moreover, it determines the slack area of key structure parameters under the specified wave condition, which provides a foundation for preliminary structure design.

The results obtained by present model show a good agreement with the observations about the dynamic tether tension in the model experiments [14,15]. As suggested in 4.1.1, with an increasing wave height, the dynamic tether tension will go though from the state of harmonic response, to the state with disturbance in the response, and to aperiodic response with occurrence of snap force finally. And the results of slack-taut map validate their conclusion that for the case of tether perpendicular to seabed (i.e. IMA = 0), slack barely occur but the inclined moored type C-30 (i.e. IMA = 30°) snap force occurs.

4.3. Slack criterion of SFT tether

In order to reveal the slack mechanism of different structure configurations, analytical approach for slack prediction is introduced instead of solving the nonlinear Equations (6) directly in this part. There are two steps to decide the occurrence of slack: firstly, to build slack criterion; secondly, to get the non-slacking SFT responses. In fact, SFT responses without considering tether slacking are sufficient to decide whether the tether would go slack or not. In this light, two reasonable assumptions are made to simplify the problem, that is:

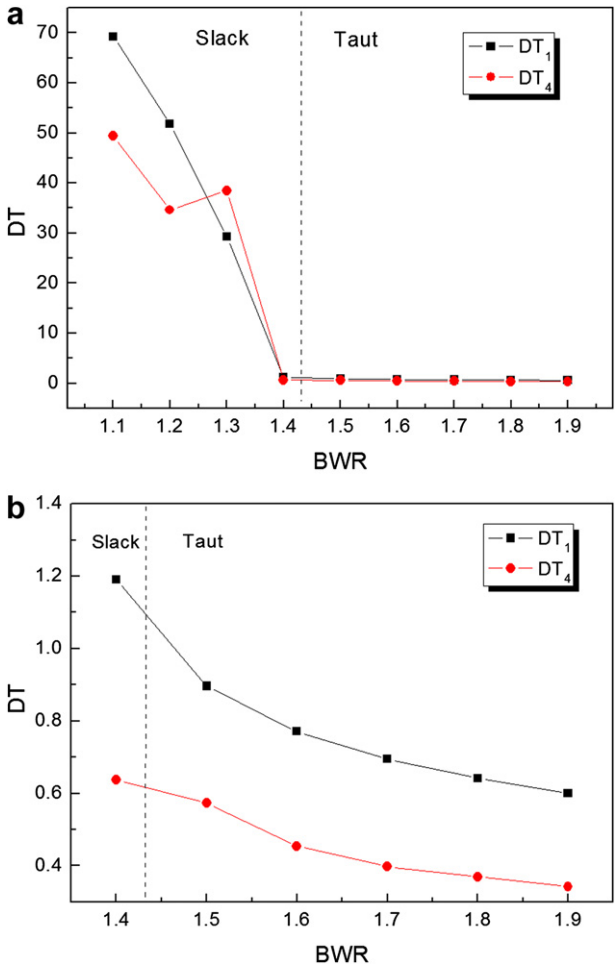

Fig. 9. Relative dynamic tension amplitude versus BWR.

I. linear tether stiffness, i.e. K_i (ΔL_i)=k.
II. neglecting SFT rotation, i.e. φ(t)=0.

Therefore following relations:$L_1(t)$=$L_4(t)$,$L_2(t)$=$L_3(t)$ hold. If SFT tethers do not go slack, $L_1(t)\geq L_n$ and $L_2(t)\geq L_n$ must be satisfied simultaneously. Expanding the expression of $L_1(t)$ and $L_2(t)$, slack criterion is given by the following inequalities:

$$\begin{cases} (x + h_2\tan\theta)^2 + (\delta y + h_2)^2 \geq \left(\dfrac{h_2}{\cos\theta + \dfrac{w}{4EA}}\right)^2 \\ (x - h_2\tan\theta)^2 + (\delta y + h_2)^2 \geq \left(\dfrac{h_2}{\cos\theta + \dfrac{w}{4EA}}\right)^2 \end{cases} \tag{9}$$

in which $\delta y = y - h_1$.

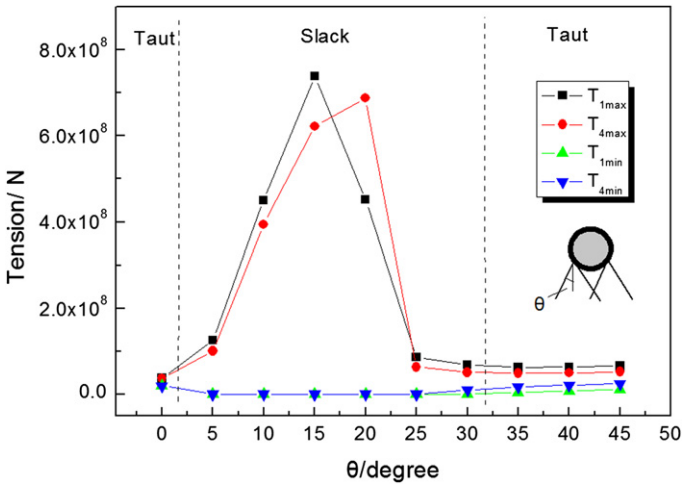

Fig. 10. Maximum and minimum tether tension force versus IMA.

SFT tether will undergo slack as long as any one of the two inequalities is not satisfied. In coordinate with x as its abscissa and δy as its ordinate, slack region is the total area of the two circles which is the shadow region as shown in Fig. 13. The slack area increases with θ and decreases with BWR. Specially, when θ is zero, the slack area is the smallest as the two circles coincide and the radii reach the minimum.

Inequalities (9) give the slack criterion of SFT tethers. Now non-slacking SFT responses are needed to determine the occurrence of tether slacking by judging the relation of SFT steady state responses with slack region. With assumptions of I, II and a small displacement relative to wave height, the terms of fluid force and restoring force are linearized to get the non-slacking response. The fluid force can be written as [17]:

$$f_x \cong (C_M + 1)\rho_w A\dot{w}_x - C_M\rho_w A\ddot{x} + \frac{1}{2}\rho_w D C_D\left(|w_x|w_x - 2|w_x|\dot{x}\right) \tag{10}$$

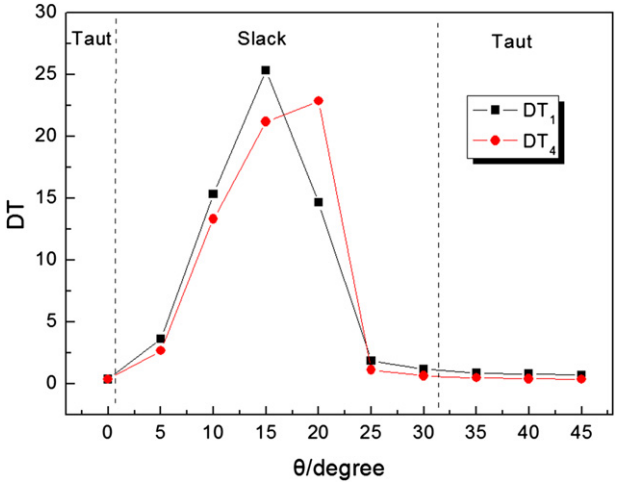

Fig. 11. Relative dynamic tension amplitude versus IMA.

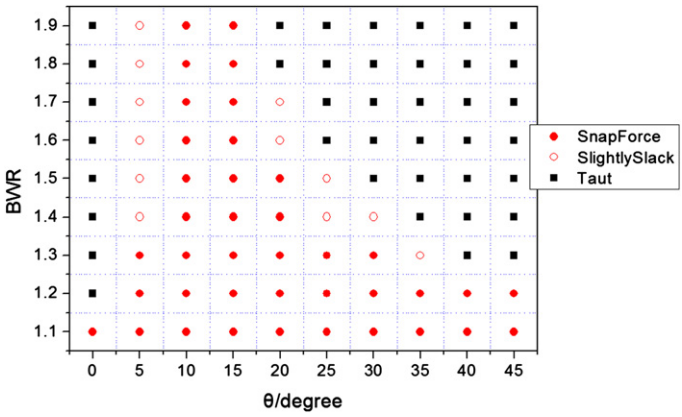

Fig. 12. The slack-taut map of SFT (wave height: 12 m, wave period: 15 s).

An average value $\hat{w}_x$ is used to approximate the instant velocity of water particle $|w_x|$. The expression of $\hat{w}_x$ is obtained by minimizing the approximation error in a least square sense. Minimizing the integral $I = \int_0^{2\pi}(|w_x|w_x - \hat{w}_x w_x)^2 \mathrm{d}(\omega t)$, we get:

$$\hat{w}_x = \frac{8}{3\pi}\frac{\omega H}{2}\frac{\cos h(ky)}{\sin h(kd)} \tag{11}$$

The fluid force is linearized as:

$$f_x \cong (C_M + 1)\rho_w A\dot{w}_x - C_M\rho_w A\ddot{x} + \overline{C}_D w_x - 2\overline{C}_D\dot{x}, \quad \overline{C}_D = \frac{1}{2}\rho_w D C_D \hat{w}_x \tag{12}$$

A similar simplification is made to f_y.

The restoring forces can be linearized in the following form :

$$\frac{1}{2}\sum_{i=1}^{4}\frac{K_i(\Delta L_i)}{a}\frac{\partial\left(\Delta L_i^2\right)}{\partial x} \cong K_x x \tag{13}$$

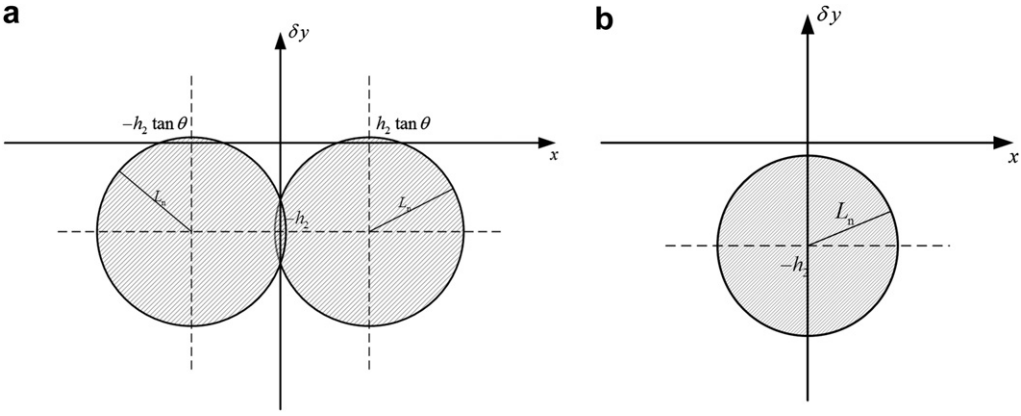

Fig. 13. Slack region of SFT. a. $\theta > 0^\circ$; b. $\theta = 0^\circ$ (Shadow area denotes the region SFT tether will go slack)

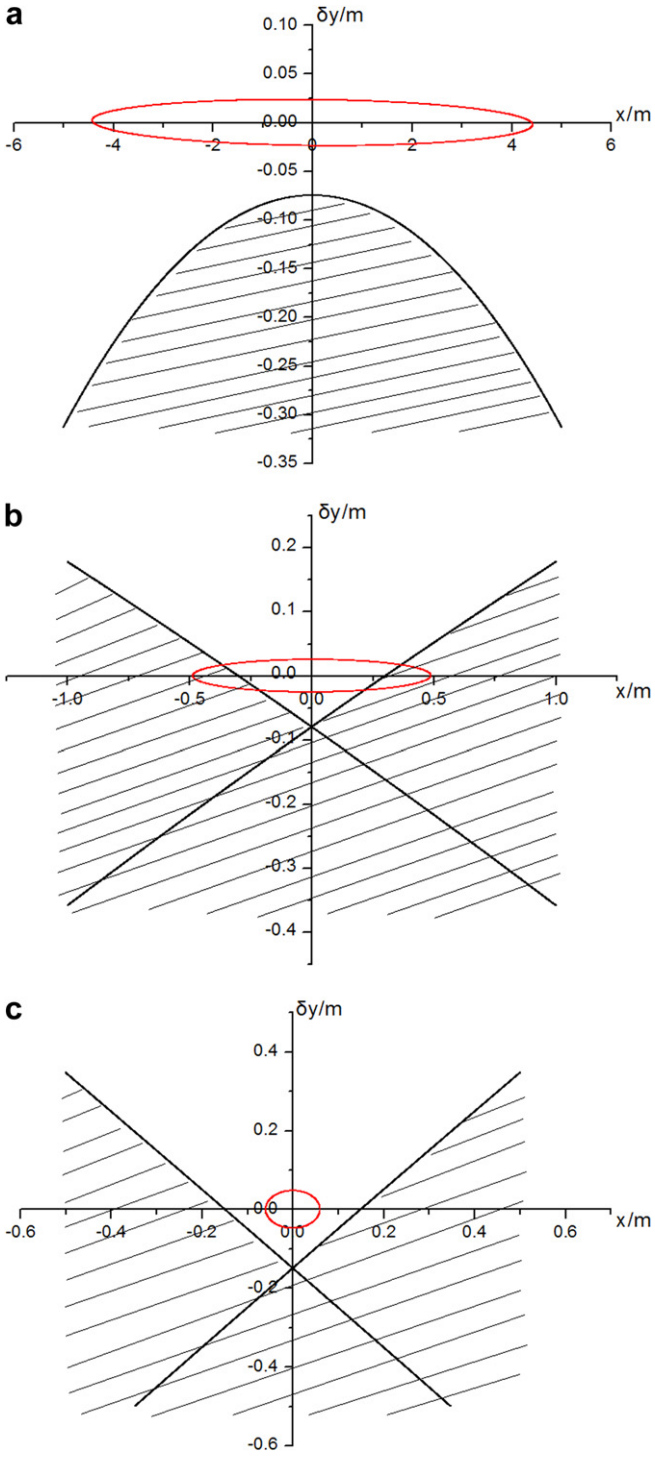

Fig. 14. Relation of non-slacking SFT responses with slack regions. a. $\theta = 0^{\circ}$; b. $\theta = 15^{\circ}$; c. $\theta = 45^{\circ}$ (Red line denotes the trajectory of SFT steady state response, and shadow area denotes the slack region. Once the steady response crosses into the slack region, the tether will go slack.) (For interpretation of the references to colour in this figure legend, the reader is referred to the web version of this article).

$$\frac{1}{2}\sum_{i=1}^{4}\frac{K_i(\Delta L_i)}{a}\frac{\partial\left(\Delta L_i^2\right)}{\partial y}\cong K_y\delta y + C_y \tag{14}$$

in which

$$K_x = \frac{4K}{a}\left[1+\frac{(h_2\tan\theta)^2 L_n}{(h_2\sec\theta)^3}-\frac{L_n}{h_2\sec\theta}\right]$$

$$K_y = \frac{4K}{a}\left[1+\frac{h_2^2 L_n}{(h_2\sec\theta)^3}-\frac{L_n}{h_2\sec\theta}\right]$$

$$C_y = \frac{4K}{a}(h_2 - L_n\cos\theta) = \frac{w}{a}$$

By using expressions (12)–(14), the governing equations are linearized as:

$$\begin{cases} \ddot{x} + 2\xi_x\omega_x\dot{x} + \omega_x^2 x = \dfrac{\alpha_x}{m^*}\sin(\omega t+\varphi_x) \\ \ddot{\delta}\, y + 2\xi_y\omega_y\dot{\delta}\, y + \omega_y^2\delta y = -\dfrac{\alpha_y}{m^*}\sin\left(\omega t+\varphi_y\right) \end{cases} \tag{15}$$

where $m^* = m/a + C_M\rho_w A$

$$\begin{cases} \alpha_x = \dfrac{\cos h(kh_1)}{\sin h(kd)}\sqrt{\left(\overline{C}_D\dfrac{\pi H}{T}\right)^2+\left[(C_M+1)\rho_w A\dfrac{2\pi^2 H}{T^2}\right]^2} \\ \tan\varphi_x = -\dfrac{\overline{C}_D\dfrac{\pi H}{T}}{(C_M+1)\rho_w A\dfrac{2\pi^2 H}{T^2}} \end{cases}$$

$$\begin{cases} \alpha_y = \dfrac{\sin h(kh_1)}{\sin h(kd)}\sqrt{\left(\overline{C}_D\dfrac{\pi H}{T}\right)^2+\left[(C_M+1)\rho_w A\dfrac{2\pi^2 H}{T^2}\right]^2} \\ \varphi_y = \varphi_x + \pi/2 \end{cases}$$

$$\omega_x = \sqrt{\frac{K_x}{m^*}},\quad \xi_x = \frac{\overline{C}_D}{m^*\omega_x},\quad \omega_y = \sqrt{\frac{K_y}{m^*}},\quad \xi_y = \frac{\overline{C}_D}{m^*\omega_y}$$

The analytical solution to governing equations (15) is available [18], and the steady state of the non-slacking response is obtained. Together with the slack criterion, a slack prediction can be easily made.

Three IMAs 0°,15°, 45° with a BWR of 1.4 are taken as examples to illustrate. Fig. 14 shows the relation of non-slacking SFT responses with corresponding slack regions. The figure indicates that even though the lateral restraint (x direction) is considerably small if θ is 0°, which induces a relatively large displacement in the lateral direction, SFT tethers still will not go slack because of the smallest slack area. If θ increases to 15°, although the lateral displacement indeed becomes much smaller than the case of an IMA of 0°, slack will occur as the slack area enlarged greatly than the case of 0°. As to the IMA of 45°, as the slack area goes large further, a relatively strong lateral restraint makes the SFT response beyond the slack region. These results coincide well with the ones showed in the slack-taut map in Fig. 12.

The example indicates that the occurrence of tether slacking is decided by the slack region and non-slacking SFT responses simultaneously. When IMA is as small as 0°, a relatively small slack region makes the slack hard to occur. When IMA increases to around 15°, an enlarged slack region makes the slack more easily to occur. If IMA continues to increase to about 45°, the occurrence of slack will be dominated by a restrained response in lateral direction and not easily to happen again.

5. Conclusions

The dynamic behaviors of SFT suffering a slack in the tethers under wave conditions are investigated numerically. The characteristics of dynamic response of SFT tether tension coincide with the observation in model experiments. The states of SFT dynamic response are categorized into three types: taut, slight slack in the tether and slack with snap force in the tether. In the cases studied, the response of SFT tether tension is more sensitive to wave height compared with wave period. BWR and IMA both have great influence on the occurrence of slack in SFT tether. A slack-taut map of SFT tethers is built at the designed wave condition with a wave height of 12 m and a wave period of 15 s. It intuitively describes the occurrences of slack and snap force with different combinations of BWR and IMA. Moreover it indicates that BWR dominates the range of influence of IMA.

The mechanism of the presented slack-taut map is revealed by introducing an analytical approach for slack prediction. Slack criterion is built and the non-slacking governing equations are solved analytically. Results indicate that the occurrence of tether slacking is dominated by the slack region and non-slacking SFT responses simultaneously, which explains the reason why the occurrence of tether slacking is rare for SFT with an IMA of 0° and 45°, but for the case of 15° is not.

Acknowledgments

This work is supported Knowledge Innovation Program of Chinese Academy of Sciences (no. KJCX2-YW-L07).

References

[1] Youshi Hong, Fei Ge, Xu Long. Researches on essential mechanics issues for submerged floating tunnel. In: Proceedings of the fifth symposium on strait crossings, 2009.
[2] FEHRL report no 1996/2a. Analysis of the submerged floating tunnel concept, in: FEHRL (Forum of European National Highway research Laboratories), Berkshire (Crowthorne): Transport Research Laboratory, 1996.
[3] Long Xu, Fei Ge, Lei Wang, Youshi Hong. Effects of fundamental structure parameters on dynamic response of submerged floating tunnel under hydrodynamic loads. Acta Mechanica Sinica 2009;25:335–44.
[4] Guojun Huang, Yingxiang Wu, Youshi Hong. Transportation of crossing waterways via Archimedes Bridge. Shipbuilding of China 2002;43:13–8.
[5] Niedzwecki JM, Thampi SK. Snap loading of marine cable systems. Applied Ocean Research 1991;13:2–11.
[6] Vassalos D, Huang S, Kourouklis A. Experimental investigation of snap loading of marine cables. In: Proceedings of the fourteenth international offshore and polar engineering conference, 2004.
[7] Plaut RH, Archilla JC, Mays TW. Snap loading in mooring lines during large three dimensional motions of a cylinder. Nonlinear Dynamics 2000;23:271–84.
[8] Huang S. Stability analysis of the heave motion of marine cable-body systems. Ocean Engineering 1999;26:531–46.
[9] Kanie S, Kokubun H, Mizutani Y. Analytical study on dynamic response of submerged floating tunnels due to wave force. In: Proceedings of the third symposium on strait crossings, 1994.
[10] Kanie S, Mikami T, Horguchi H, Miyauchi N. Effect of nonlinearity in restoring force on dynamic response of SFT. In: Proceedings of the fourth symposium on strait crossings, 2001.
[11] Sato M, Kanie S, Mikami T. Mathematical analogy of a beam on elastic supports as a beam on elastic foundation. Applied Mathematical Modeling 2008;32:688–99.
[12] Fogazzi P, Perotti F. The dynamic response of seabed anchored floating tunnels under seismic excitation. Earthquake Engineering and Structural Dynamics 2000;29:273–95.
[13] Di Pilato M, Perotti F, Fogazzi P. 3D dynamic response of submerged floating tunnels under seismic and hydrodynamic excitation. Engineering Structures 2008;30:268–81.
[14] Kunisu H, Mizuno S, Mizuno Y, Saeki H. Study on submerged floating tunnel characteristics under the wave condition. In: Proceedings of the fourth international offshore and polar engineering conference, 1994.
[15] Mizuno S, Tada A, Mizuno Y, Kunisu H, Yamashita T, Saeki H. Experimental study on characteristics of submerged floating tunnels under regular waves. In: Proceedings of the third symposium on strait crossings, 1994.
[16] Maeda N, Morikawa M, Ishikawa K, Kakuta Y. Study on structural characteristics of support systems for submerged floating tunnel. In: Proceedings of the third symposium on strait crossings, 1994.
[17] Dawson TH. Offshore structural engineering. Englewood Cliff, NJ: Prentice-Hall; 1983.
[18] Clough RW, Penzien J. Dynamics of structures. 3rd ed. Berkeley: Computers and Structures, Inc.; 1995.